THE C, N, AND O ABUNDANCES OF GIANT STARS IN ω CENTAURI[1]

J. G. COHEN
California Institute of Technology

AND

R. A. BELL
Astronomy Program, University of Maryland
Received 1985 August 9; accepted 1985 December 4

ABSTRACT

Indices measuring the strength of CH, C_2, CN, and NH bands and Ca II and Ca I lines have been determined for 72 stars in ω Cen. These data, and narrow-band photometry of the 2.4 μm CO bands, are calibrated by using theoretical indices derived from synthetic spectra which are computed via a grid of model atmospheres of appropriate parameters.

In addition to the four C stars, we find two groups of giants in ω Cen. Both groups include stars spanning a wide range of abundances of the heavy elements, Z. The N-enhanced stars have N/Z enhanced by a factor of 5 to 15, while both C/Z and O/Z are depleted by a factor which may be as much as 10. This depletion allows the CH and CO features to be fitted satisfactorily and yields enough nitrogen to fit CN and NH features. The N-normal stars have N/Z and C/Z within factor of 2 of solar. The range of variation of C and N is typical of those seen in other globular clusters.

Subject headings: clusters: globular — stars: abundances — stars: evolution — stars: late-type

I. INTRODUCTION

It is well established that the globular cluster ω Cen is unique among the galactic globulars. It possesses a wide giant branch in the luminosity–effective temperature plane (see, for example, Woolley *et al.* 1966 or Cannon and Stobie 1973). Spectra of individual giants (Cohen 1981; Mallia and Pagel 1981; Gratton 1982), of RR Lyrae variables (Freeman and Rodgers 1975), and of turn-off region stars (Hesser *et al.* 1985) have all demonstrated that there is a wide range in metal abundance among the ω Cen stars. Persson *et al.* (1980) (henceforth PFCAM) showed that there is a wide range in strength of the 2.3 μm CO band at a given $V - K$ color (i.e. a given T_{eff}).

The purpose of this paper is to explore the abundances of the light elements C, N, and O in the ω Cen giants and to compare the results with theoretical predictions and with the results for stars in other extensively studied globular clusters which are uniform in heavy element abundances. The observational data are presented in § II. Correlations among the measured indices for various molecular and atomic absorption features are described in § III, while § IV presents a calibration of the observed indices derived from spectral synthesis techniques applied to model atmospheres of varying T_{eff}, gravity, metallicity, and C, N, and O abundances. The implications of the variations in light element abundances are discussed in § V. A summary of the important conclusions is presented in § VI.

II. OBSERVATIONS

A sample of 82 stars on the upper giant branch (GB) of ω Centauri was studied in the infrared by PFCAM. Ignoring the large amplitude variables, we have observed all the stars on their list with measured CO indices, plus the brighter of those without CO indices, to form the sample of 72 program stars.

Radial velocity measurements suggest that all these stars are members. These observations were made with the intensified Reticon detector (Shectman 1978) at the Cassegrain focus of the 2.5 m Du Pont telescope of the Las Campanas Observatory mainly in 1980 May, but with a few additional scans in 1981 May. Two observations were obtained for most of the stars. The first, at a resolution of 1.4 Å (corresponding to the FWHM of the detector of 3.5 pixels) covered the wavelength region from 3700 to 4800 Å. These are the observations which were used to obtain the radial velocities. The second, at a lower resolution of 4.0 Å, covered the region from 3000 to 5000 Å, with a filter strongly suppressing the region longward of 4000 Å. Observations were made by alternating the star between each pair of apertures, separated in declination, so that all the scans were fully sky subtracted. Scans of a tungsten lamp were made to remove pixel-to-pixel variations, while wavelength calibration was achieved using noble gas arcs.

The seeing was significantly better than the width of the aperture (2″) on all nights. However, the spectra were not fluxed. To remove the curvature in the continuum, at least approximately, a third-order polynomial was computed as a fit to the counts within the intervals listed in Table 1a; this fit was then used to produce a crudely flattened continuum. Because of the very steep drop-off in continuum signal induced by the long pass cutoff of the filter near the 4700 Å C_2 band, the continuum for this feature only was represented by a linear interpolation over the bandpass 4575–4610 Å and 4670–4810 Å on either side of the C_2 band. The continuum intervals were in all cases chosen to avoid strong atomic or molecular features as much as possible. Of course, especially at wavelengths shortward of 4300 Å, it becomes impossible to avoid all features completely in the more metal-rich ω Cen stars.

Indices were then determined for the bands of CH, CN, and NH within the spectral range covered on the low- and high-resolution scans. These were defined from the sky-subtracted, roughly flattened count rates (c_i) by averaging over appropri-

TABLE 1

BANDPASSES FOR CONTINUUM FLATTENING

Index	Bandpass (Å)	Bandpass (Å)
A. Low Dispersion		
C$_2$	4575–4610	4760–4810
NH, CN	3300–3330	3890–3910
	3485–3505	4025–4050
	3670–3690	
B. High Dispersion		
CN, CH, H + K, Ca I	3770–3785	4335–4336
	3890–3910	4345–4346
	3990–4010	4365–4366
	4087–4088	4396–4397
	4093–4094	4402–4403
	4221–4222	4448–4449
	4244–4245	4477–4478

ate wavelength bandpasses (which process we denote by A). In general, each index was defined by

$$I = 1 - \frac{A(c_i, \lambda_1 - \lambda_2)}{aA(c_i, \lambda_3 - \lambda_4) + bA(c_i, \lambda_5 - \lambda_6)},$$

where the two wavelength intervals $\lambda_3 - \lambda_4$ and $\lambda_5 - \lambda_6$ represent continuum intervals, and $\lambda_1 - \lambda_2$ is the molecular feature of interest. The continuum weights a and b were chosen so as to minimize the effects of any artificial continuum slope such as could result, for example, from varying amounts of spillover beyond the aperture width due to differential refraction. These weights and the bandpasses are listed for each index in Table 2. The actual wavelength intervals used were obtained from those tabulated by applying a radial velocity correction of 230 km s^{-1} (Webbink 1981) for all the ω Cen stars.

This approach could not be used for the 4226 Å feature of Ca I owing to the adjacent CN and CH bands. For this feature, a pseudo-equivalent width was measured from the high-dispersion scans using a bandpass of 4222–4232 Å. The continuum was defined as above, by fitting a third-order polynomial to selected wavelength intervals listed in Table 1b; appropriate radial velocity shifts in the intervals were again made.

A minimum total count of 1000 was always obtained for the continuum bandpass to the blue of the NH feature; all other wavelength intervals had considerably higher net counts. The

TABLE 2

FEATURES AND WEIGHTS OF THE INTERVALS FOR INDICES

FEATURE	FEATURE BAND (Å)	SIDE BAND (Å)	SIDE BAND (Å)	WEIGHTS a	b
A. High Dispersion					
CH	4290–4320	4350–4370	4235–4270	0.5	0.5
CN	4160–4210	4115–4130	4235–4270	0.5	0.5
uvCN	3830–3880	3890–3910	3770–3785	0.5	0.5
H + K	3920–3980	3890–3910	3990–4010	0.5	0.5
B. Low Dispersion					
NH	3350–3420	3485–3505	3318–3330	0.33	0.67
Low CN	3820–3870	3900–3910	3650–3700	0.67	0.33
C$_2$	4660–4720	4760–4800	4575–4610	0.5	0.5

principal uncertainty is not in the count rates within any bandpass themselves, but rather in the measurement of indices in the absence of fluxed spectra. This resulting uncertainty in the tabulated indices is believed to be $\pm 4\%$; the pseudo-equivalent width of the 4226 Å feature of Ca I has a larger uncertainty of $\pm 10\%$. The two independent measurements of the 3883 Å CN band, one from the low and one from the high-dispersion scans, indicate the good accuracy of these measurements. Duplicate scans of five stars also support the claimed high accuracy of these molecular indices.

The star RGO 300 is a radial velocity member of ω Cen with TiO and ZrO bands classified S2 by Lloyd-Evans (1983). Our three spectra reveal the presence of a hot companion which is contributing significantly to the total light at wavelengths of 4000 Å and below. The higher Balmer lines and a strong uv continuum are seen, and the Ca II–H$_\epsilon$ blend is stronger than the 3933 Å Ca II line. Consequently, we do not consider this star further in the present paper and its indices are omitted from all the figures.

The measured molecular indices and atomic line strengths for the 72 program stars are given in Table 3.

III. THE CORRELATIONS OF THE MOLECULAR BAND INDICES AND ATOMIC LINE STRENGTHS

The displacement of a star in the M_V, $V - K$ diagram with respect to the M92 fiducial giant branch at the same m_{bol} was used by PFCAM to define the parameter $R(V - K)$; observationally, $R(V - K)$ is equal to 0.71 for a star with the metallicity of an M71 star. We use this parameter to separate the stars in metallicity. In order to have metallicity values available for subsequent use we adopt $[M/H] = -2.1$ dex for M92 $[R(V - K) = 0.0]$ and $[M/H] = -0.8$ dex for M71 $[R(V - K) = 0.71]$ (Cohen 1983; Bell and Gustafsson 1983). For M13, $R(V - K) = 0.3$, and we adopt $[M/H] = -1.5$ dex (Cohen 1978; Bell and Dickens 1980). This separation in metallicity given by the $R(V - K)$ parameter is supported by the high-dispersion analyses of several ω Cen members by Cohen (1981), Mallia and Pagel (1981), and Gratton (1982), as well as by the trends in line strength shown by the atomic features as displayed subsequently here.

The figures are separated into three panels covering the three metallicity ranges: the most metal-poor ω Cen stars $[R(V - K) < 0.20]$, the intermediate metallicity giants $[0.20 \le R(V - K) \le 0.40]$, and the high metallicity giants $[R(V - K) > 0.40]$. The abundances which correspond to these three groups are taken to be -2.0, -1.5, and -1.0 dex respectively, based on the discussion above. Because atomic and molecular line strengths depend on both T_{eff} and metallicity (as well as surface gravity), such a complex display of the data becomes necessary.

We first consider the C$_2$ bands. Only four stars have a C$_2$ index greater than 10%; the C$_2$ indices of the remaining stars fluctuate about zero. RGO 55 and RGO 70 are well known CH stars (Harding 1972; Dickens 1972), while RGO 577 was found by this survey to have strong C$_2$ bands; unpublished observations by Zinn and Norris also had independently found this star to be a carbon star. RGO 577 is a radial velocity member of the globular cluster, with M_{bol} (from PFCAM) of -1.45 mag, well below that of the tip of the giant branch. RGO 279 is also a carbon star, with weaker C$_2$ bands and a smaller value of C/O. A fifth carbon star was found by Bond (1975), near the cluster center. Models for these carbon-rich objects have not yet been computed, and the observations are

TABLE 3

INDICES OF ω CENTAURI STARS

RGO (#)	(V-K)$_o$ (mag)	CO (mag)	CH (%)	CN (%)	UVCN (%)	LOCN (%)	NH (%)	C$_2$ (%)	H+K (%)	CaI (A)	Group
Low Metallicity Group											
40	3.14	0.095	0.228	0.085	0.328	0.345	0.175	0.028	0.412	1.88	L
46	3.41	0.040	0.210	0.039	0.140	0.188	0.097	-0.037	0.445	2.78	U
48	3.40	0.040	0.226	0.057	0.176	0.200	-0.040	-0.004	0.394	1.69	U
49	3.34	0.060	0.229	0.066	0.102	0.145	0.147	0.025	0.375	1.93	L
55	3.49	0.060	0.150	0.484	0.735	0.786	0.067	0.663	0.189	-0.78	C
58	3.14	0.020	0.203	0.058	0.214	0.222	0.257	-0.040	0.437	1.71	U
61	3.48	0.050	0.216	0.047	0.192	0.221	0.197	-0.068	0.369	2.55	U
62	3.43	0.070	0.193	0.079	0.192	0.245	-0.032	-0.015	0.411	2.24	L
70	3.42	0.150	0.219	0.365	0.690	0.699	0.164	0.309	0.335	1.56	C
74	3.03	0.035	0.195	0.044	0.221	0.202	0.253	0.034	0.432	1.50	U
102	3.17	0.015	0.187	0.058	0.164	0.216	0.192	-0.029	0.414	1.61	U
124	3.09	0.060	0.195	0.028	0.189	0.214	0.177	-0.062	0.451	1.79	L
159	2.97	0.040	0.222	0.033	0.147	0.141	0.170	-0.043	0.414	1.65	U
180	2.76	0.035	0.189	0.020	0.007	0.070	0.155	-0.035	0.362	1.44	U
213	2.67	0.010	0.218	0.000	0.047	0.080	0.150	-0.074	0.379	0.49	U
234	2.70	0.010	0.171	0.021	0.041	0.088	0.201	-0.036	0.362	1.45	U
256	2.80	0.001	0.203	0.036	0.262	0.256	0.275	-0.043	0.422	1.19	U
269	2.79	0.025	0.208	0.018	0.072	0.129	0.107	-0.104	0.451	1.23	U
279	2.81	0.105	0.245	0.236	0.595	0.587	0.165	0.135	0.343	1.07	C
364	2.57	0.001	0.209	0.020	0.141	...	...	...	0.373	0.52	U
402	2.53	0.005	0.123	0.043	0.147	0.113	0.295	-0.018	0.351	0.00	U
415	2.50	0.015	0.237	0.022	0.236	...	...	...	0.355	0.96	U
461	2.61	0.055	0.240	0.069	0.415	...	...	...	0.445	1.67	L
462	2.40	...	0.122	0.026	0.084	...	...	...	0.354	0.80	U
483	2.56	0.015	0.175	-0.010	0.088	...	...	...	0.357	0.68	U
509	2.53	...	0.174	0.028	0.168	...	...	...	0.374	1.40	U
G318	2.40	...	0.259	0.053	0.342	...	...	...	0.377	0.85	U
5941	2.16	...	0.149	0.020	-0.010	...	...	...	0.271	0.48	U
6113	2.25	...	0.201	0.044	0.246	...	...	...	0.377	0.93	U
Intermediate Metallicity Group											
43	3.60	0.140	0.228	0.145	0.284	0.334	0.166	0.025	0.446	2.62	L
53	3.62	0.105	0.189	0.079	0.197	0.252	0.207	0.071	0.431	2.15	L
56	3.53	0.060	0.225	0.144	0.279	0.374	0.236	0.003	0.457	2.74	U
84	3.68	0.180	0.221	0.076	0.275	0.326	0.253	-0.002	0.511	4.02	L
90	3.46	0.045	0.230	0.077	0.215	0.310	0.317	-0.034	0.466	2.88	U
91	3.14	0.015	0.206	0.031	0.143	0.170	0.144	0.002	0.419	1.43	U
96	3.26	0.050	0.219	0.038	0.125	0.171	0.068	-0.019	0.432	2.22	U
132	3.72	0.155	0.229	0.107	0.259	0.304	0.140	0.021	0.466	3.24	L
139	3.17	0.135	0.235	0.202	0.510	0.539	0.282	-0.029	0.440	1.92	L
150	3.53	0.070	0.215	0.209	0.363	0.438	0.286	0.050	0.574	3.82	W
155	3.11	0.075	0.235	0.055	0.248	0.266	0.184	0.033	0.428	2.42	L
161	3.03	0.070	0.229	0.027	0.255	0.265	0.199	-0.002	0.406	2.10	L
171	3.28	0.145	0.234	0.081	0.287	0.338	0.214	-0.007	0.487	3.05	L
253	2.93	0.005	0.223	0.229	0.561	0.582	0.312	-0.047	0.477	2.16	U
272	2.96	0.085	0.235	0.100	0.402	0.426	0.192	-0.053	0.461	1.79	L
287	3.01	0.150	0.257	0.119	0.411	0.434	0.194	0.016	0.485	2.50	L
297	2.85	0.085	0.246	0.048	0.313	0.350	0.241	-0.025	0.440	2.12	L
312	2.90	0.065	0.237	0.041	0.308	...	...	...	0.440	1.35	L
320	3.80	0.300	0.192	0.086	0.136	0.209	0.117	-0.010	0.410	4.58	L
394	2.92	0.105	0.248	0.170	0.483	0.505	0.298	0.004	0.509	2.49	L
464	2.65	0.070	0.249	0.024	0.299	0.245	0.194	0.057	0.374	1.34	L
465	2.87	0.050	0.246	0.194	0.493	0.531	0.352	-0.048	0.495	2.35	W
472	2.84	0.135	0.260	0.079	0.374	...	...	...	0.510	2.44	L
480	2.80	0.060	0.256	0.318	0.626	0.672	0.279	0.021	0.572	2.77	W
505	2.87	0.045	0.244	0.272	0.547	0.647	0.328	-0.017	0.560	2.95	W
537	2.74	0.100	0.253	0.040	0.390	...	...	...	0.460	1.19	L
557	2.82	0.055	0.246	0.272	0.619	0.694	0.386	0.001	0.518	2.34	W
577	2.71	0.120	0.134	0.262	0.606	0.665	0.037	0.467	0.243	-0.65	C

TABLE 3—*Continued*

RGO (#)	(V-K)$_o$ (mag)	CO (mag)	CH (%)	CN (%)	UVCN (%)	LOCN (%)	NH (%)	C$_2$ (%)	H+K (%)	CaI (A)	Group
High Metallicity Group											
162	3.52	0.080	0.228	0.267	0.459	0.529	0.251	0.002	0.541	3.22	W
179	3.76	0.195	0.217	0.079	0.276	0.313	0.233	0.022	0.532	4.73	L
201	3.88	0.230	0.233	0.127	0.241	0.322	0.125	0.033	0.508	4.69	L
219	3.43	0.180	0.233	0.096	0.309	0.337	0.159	-0.024	0.493	3.49	L
231	3.45	0.080	0.241	0.183	0.239	0.415	0.235	-0.018	0.522	4.35	W
248	3.72	0.100	0.232	0.183	0.377	0.395	0.244	0.037	0.554	4.64	W
270	3.26	0.200	0.225	0.132	0.343	0.434	0.211	-0.046	0.489	3.36	L
300	3.62	0.155	0.163	0.103	0.101	0.197	0.050	0.039	0.280	4.74	.
357	3.47	0.130	0.258	0.215	0.377	0.441	0.247	0.017	0.555	5.04	W
421	3.02	0.060	...	...	...	0.611	0.279	0.005	...	...	W
451	3.31	0.110	0.204	0.183	0.352	0.428	0.185	-0.002	0.492	4.09	W
371	3.45	0.105	0.218	0.179	0.317	0.468	0.222	0.049	0.561	4.28	W
425	3.99	0.155	0.210	0.148	0.213	0.334	0.131	0.025	0.578	5.56	W
447	3.94	0.110	0.205	0.145	0.220	0.328	0.227	-0.009	0.518	5.94	W
513	3.99	0.145	0.205	0.142	0.301	0.351	0.377	-0.016	0.587	5.96	W

not discussed in detail. However, we note that both RGO 279 and 577 have very strong CN bands, similar to those seen in RGO 55 and 70. The synthetic spectra of Bell and Dickens (1974) show that strong CN occurs in CH stars even if the nitrogen abundance is not enhanced. Not all stars with very strong CN are CH stars, however, and RGO 253 has very strong CN bands and negligible C$_2$ and CO.

The CO indices of all the stars have been measured by PFCAM. In their Figure 5, stars classified into three groups. In the first, denoted in the final column of Table 3 as "L" (and plotted as open squares), PFCAM argued that the CO index was abnormally large for the metallicity and T_{eff} of the star, Such stars are on the more vertical sequence of Figure 5 of PFCAM. There is also a group of stars with weaker CO indices for their metallicity and temperature, denoted "W" in the last column of Table 3 and plotted as filled circles. In the lowest metallicity or the hottest stars, the CO band is so weak that no separation of the two groups can be achieved. Such stars, plus four of the hotter stars which have no CO measurements, are denoted "U" in the last column of the table and are always plotted as open circles. The four carbon stars are denoted by C in the tables and plotted as stars. It is clear that the C/O ratio in the CH stars varies from one another. For example, RGO 55 and 70 have the same $V - K$ color (and therefore the same temperature), but RGO 70 has much stronger CO and weaker C$_2$ and therefore a much lower C/O ratio.

The CO band indices are plotted as a function of reddening corrected $(V - K)_0$ color in Figure 1a–c; the symbols are as defined above. These bands show a great range in strength even when the stars are separated into the different abundance groups. In the lowest abundance group, the range is largely caused by the presence of the CH stars RGO 70 and 279, both of which have very strong CO for this group. However, the two normal giants RGO 40 and 461 also have larger CO indices than the other stars of the same $V - K$ color in the group. PFCAM also drew attention to the fact that many of the ω Cen giants have very strong CO compared with stars in other clusters. Examples of these stars are RGO 170, 201, 219, and 270. The possibility that these stars are simply extremely metal rich will be examined later. In all the clusters observed by Frogel, Persson, and Cohen (1983), stars with CO bands of this

strength at $V - K$ color near 3.5 mag are seen only in NGC 5927. All the 47 Tuc stars have weaker CO.

In Figure 2a–c we plot the CH index as a function of the reddening corrected $(V - K)_0$ color for the 72 stars. The symbols are as defined above. Figure 3 is completely analogous for the 4200 Å CN band, while the mean of two independent measurements of the 3883 Å CN band is shown in Figure 4. The behavior of the NH index in ω Cen giants is displayed in Figure 5. Figure 6a–c presents the H + K indices as a function of T_{eff} for the three metallicity bins, while Figure 7a–c does so for the pseudo-equivalent width of the 4226 Å Ca I feature.

The CH indices plotted in Figure 2 show no separation between the CO-strong and CO-weak groups of ω Cen giants. Furthermore, there is at best only a slight increase in the mean CH index at a fixed T_{eff} as the mean metallicity increases. Excluding the CH stars, while there may be a range in the strength of the CH band among the ω Cen giants, it is not a large one.

Norris and Bessell (1975) and Dickens and Bell (1976) showed that the CN bands have a truly impressive range of strengths among ω Cen stars. Figures 3 and 4 also show the great range in CN among stars of the same T_{eff} and metallicity group. There are many stars which do not show detectable C$_2$ bands and yet have CN bands as strong as those of the carbon stars. It is also clear from Figures 3 and 4 that within each metallicity group, the CO strong stars have generally weaker CN than their counterparts at the same T_{eff} among the CO weak stars. The CN band strengths reached by some of the ω Cen giants, even those from only the two lowest metallicity groups, are truly phenomenal. They exceed the strength of the CN bands in even the CN-strong 47 Tuc stars, a few of which were observed and reduced in the same manner as the ω Cen giants.

The NH bands also show a considerable variation in strength among the ω Cen stars. In general, the stronger NH bands within each panel of Figure 5 are found among the group of CO weak stars.

To summarize, for stars of a given T_{eff} and heavy element metallicity, (1) CN strength is in general stronger in the CO weak stars; (2) NH strength is stronger in the CO weak stars; (3) CH does not vary much.
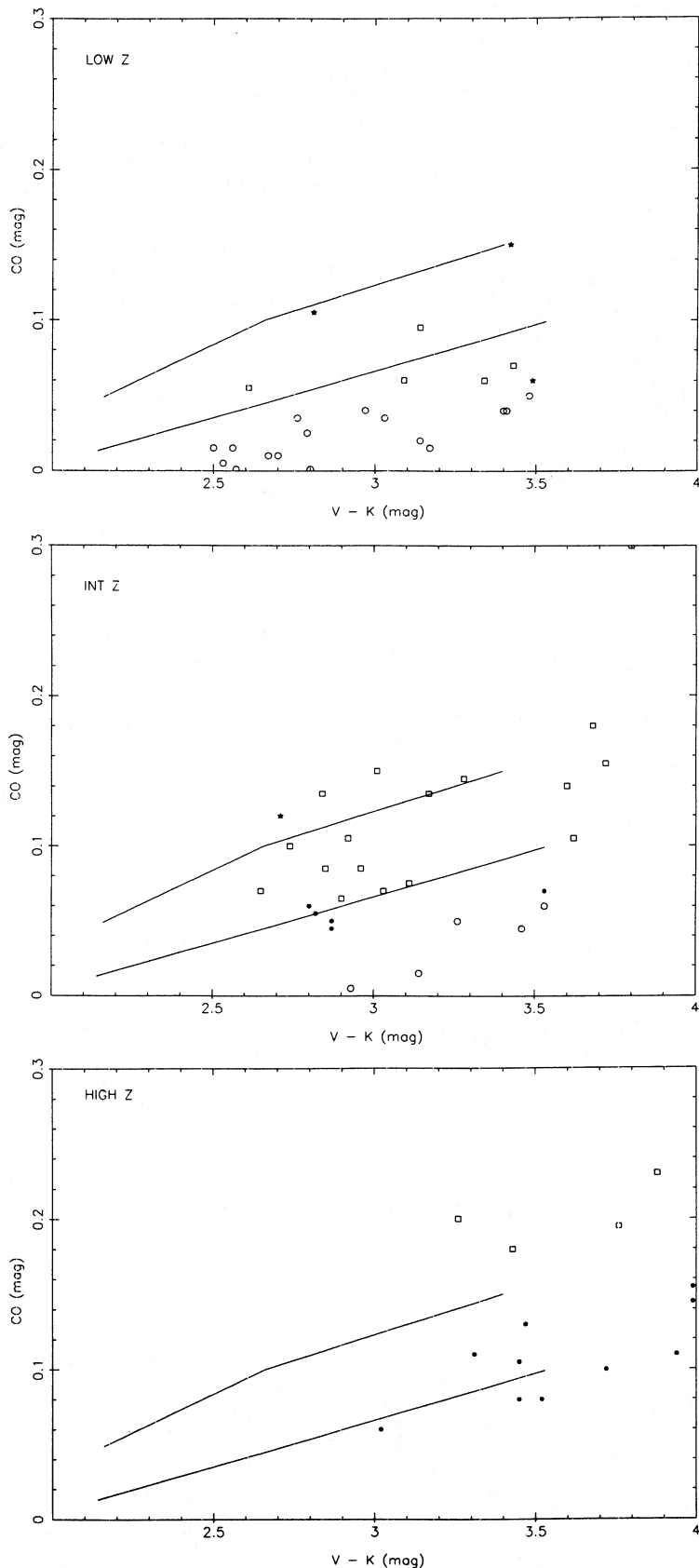
FIG. 1.—The indices of the strength of the 2.4 μm CO band from PFCAM for ω Cen stars are shown as a function of unreddened $V - K$ color. The three panels display the low, intermediate, and high metallicity groups of the sample of ω Cen giants. The four carbon stars are indicated by asterisks. The filled circles denote the CO weak–CN strong stars, while the open squares are the CO strong–CN weak stars. The open circles are the hotter stars or those of very low metallicity with such weak CO bands that no separation of the two groups is possible. The two solid lines connect the CO indices predicted by the synthetic spectra computed from model atmospheres at T_{eff} = 4000, 4500, and 5000 K and of metallicity of 1/10 and 1/100 solar. The surface gravities of the model atmospheres at each T_{eff} correspond to globular cluster giants of the appropriate metallicity.
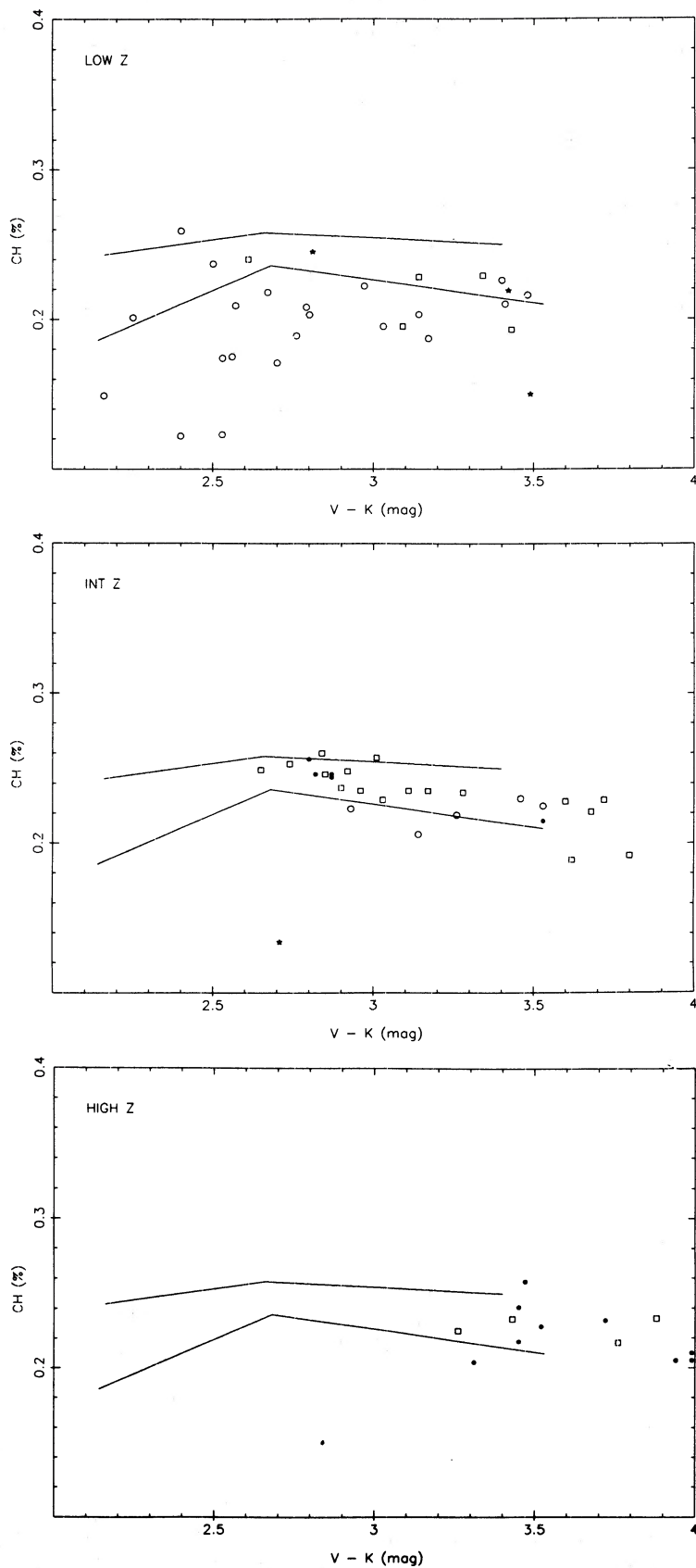
FIG. 2.—The indices for the strenth of the 4300 Å CH band for ω Cen stars are plotted as a function of unreddened $V - K$ color. The symbols are as in Fig. 1. The solid lines represent the CH indices predicted from model atmospheres appropriate to globular cluster giants with metallicities of 1/10 and 1/100 solar as in Fig. 1.
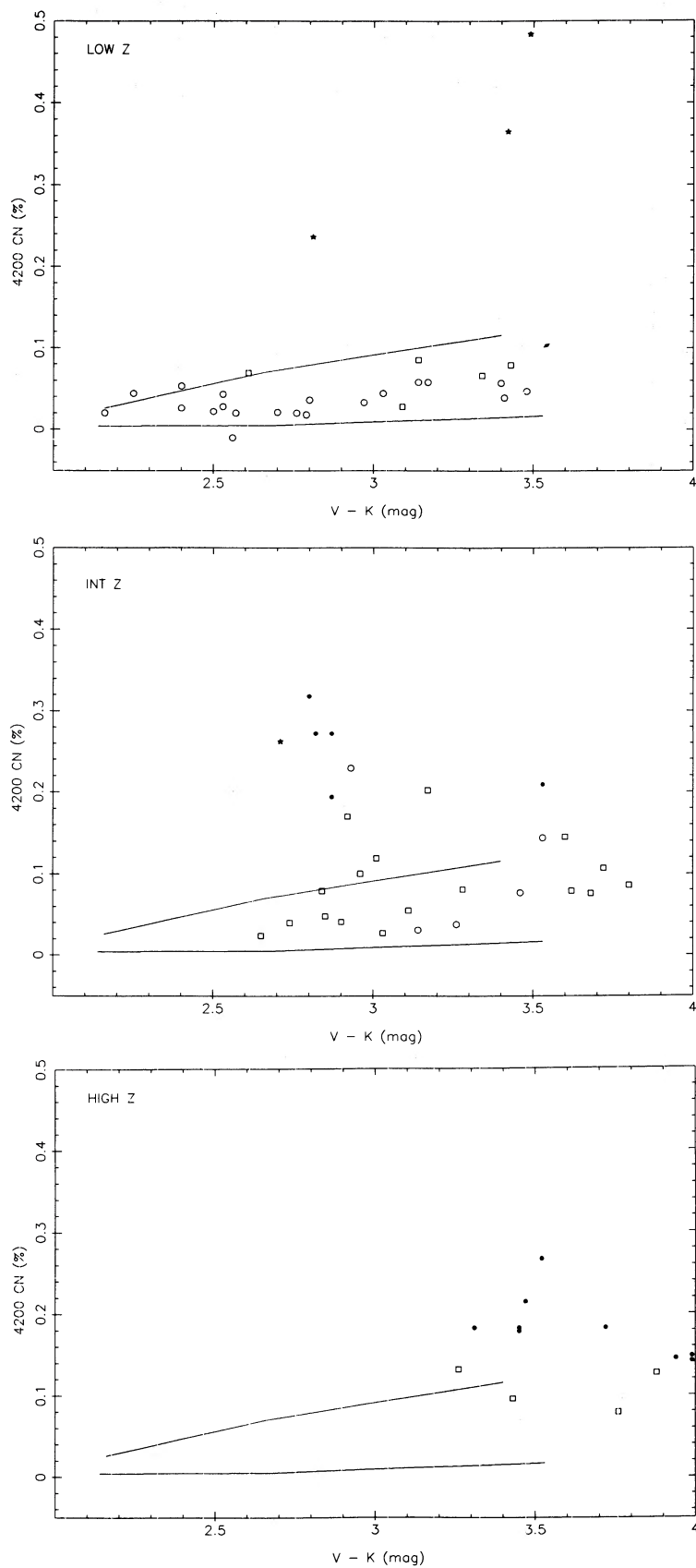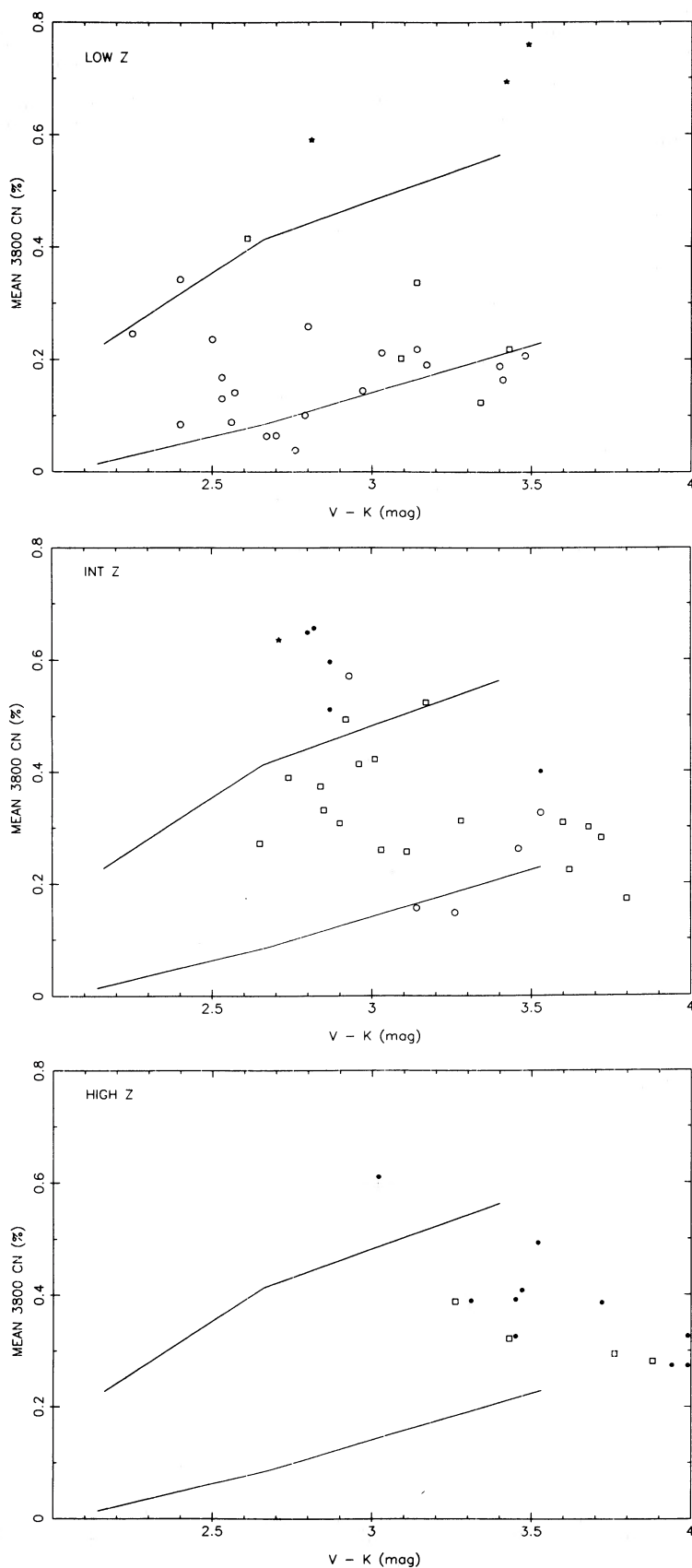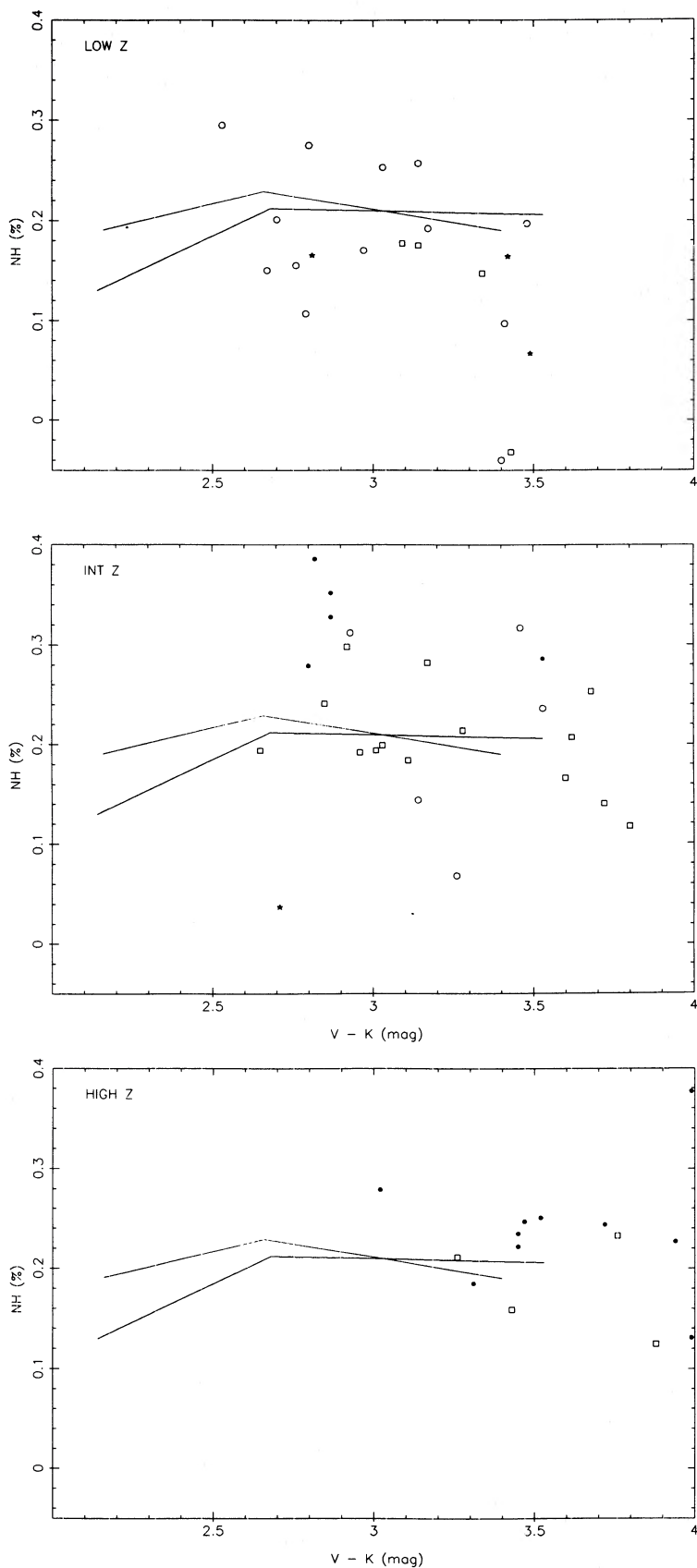
703

Fig. 3.—The indices of the strength of the 4200 Å CN band in a sample of ω Cen stars are displayed as a function of unreddened $V - K$ color. The symbols are as in Fig. 1. The solid lines represent the CN indices predicted from model atmospheres appropriate to globular cluster giants with metallicities of 1/10 and 1/100 solar.

704

FIG. 4.—The mean of two independent measurements of the strength of the 3883 Å CN band in ω Cen stars is plotted as a function of unreddened $V-K$ color. The symbols are as in Fig. 1. The solid lines display the mean of the two predicted CN indices from model atmospheres appropriate for globular cluster giants with metallicities of 1/10 and 1/100 solar.

705

Fig. 5.—The indices of the strength of the 3360 Å NH band is a sample of ω Cen giants is shown as a function of unreddened $V - K$ color. The symbols are as in Fig. 1. The solid lines represent the NH indices predicted from model atmospheres appropriate for globular cluster giants with metallicities of 1/10 and 1/100 solar.
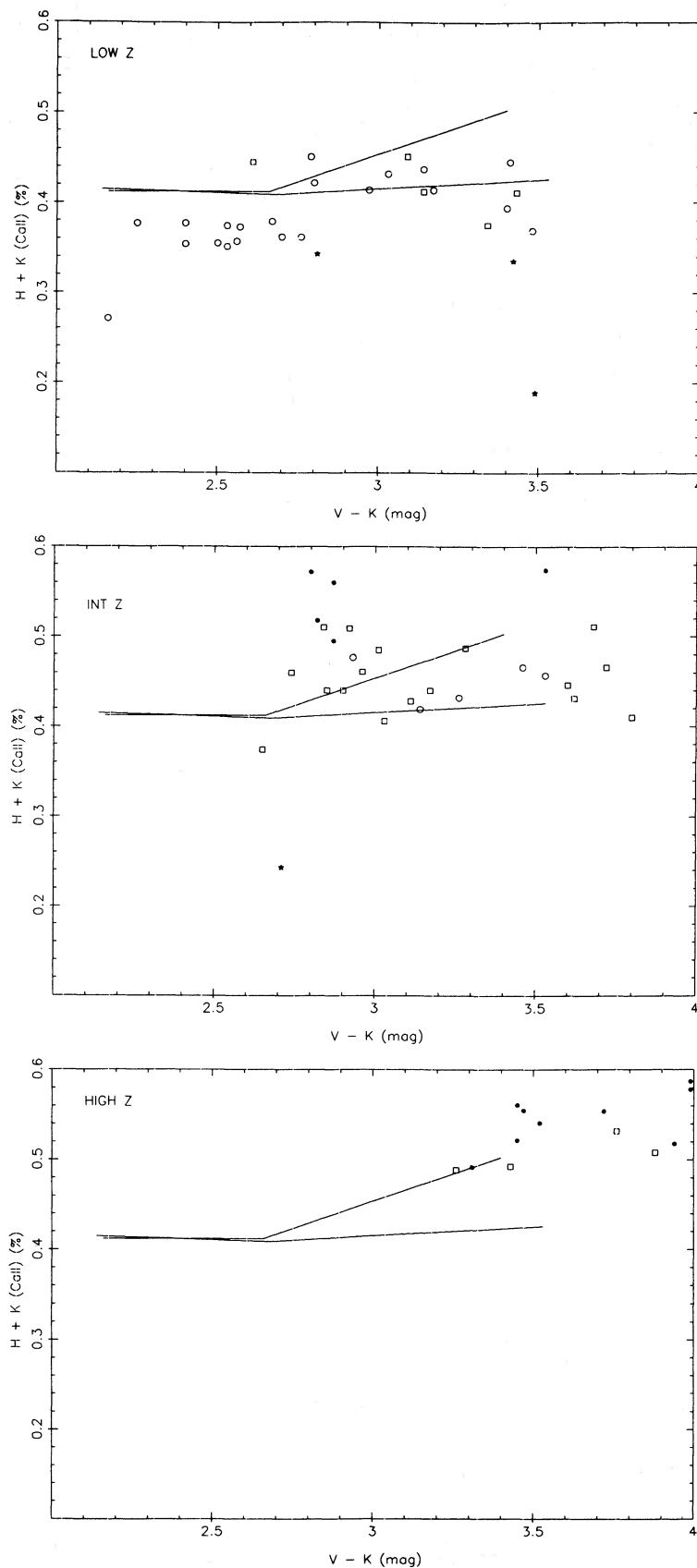
Fig. 6.—The H + K indices of the strength of the Ca II resonance lines are shown as a function of unreddened $V - K$ color for a sample of ω Cen stars. The symbols are identical to those in Fig. 1. The solid lines represent the predicted H + K indices from model atmospheres appropriate to globular cluster red giants of 1/10 and 1/100 solar metallicity.
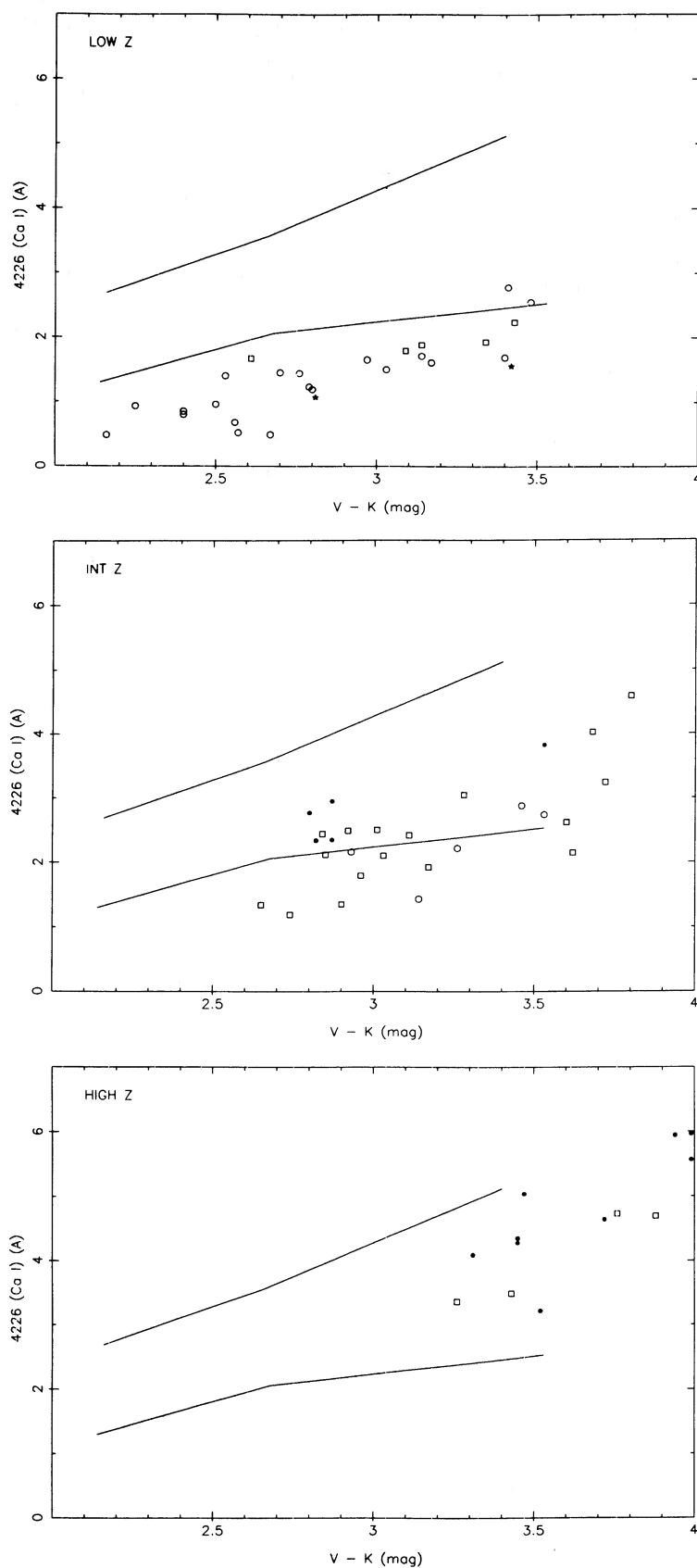
707

FIG. 7.—The pseudo-equivalent width of the 4226 Å Ca I feature is displayed as function of unreddened $V - K$ color for a sample of ω Cen stars. The symbols are as in Fig. 1. The solid lines represent the predicted strength of the Ca I feature calculated from model atmospheres appropriate to globular cluster giants of 1/10 and 1/100 solar metallicity.

IV. CALIBRATION OF THE INDICES

It is known that in several of the globular clusters, including M92 and NGC 6397, the most luminous stars are depleted in carbon. It is commonly believed that this depletion results from the mixing of nuclear processed material from the stellar interior to the surface. However, in addition to material depleted in carbon, it is also possible for material depleted in oxygen to be mixed to the surface as well. The relative abundances of carbon, nitrogen, and oxygen are such that minor depletions result in significant enhancement of nitrogen. The question then arises as to whether it is possible for values of C, N, and O to be chosen such that the observed CH, CO, and NH band strengths in the ω Cen giants can be reproduced simultaneously. Once complicating factor (which we ignore here) is whether the difference in isotope ratios from star to star is significant.

a) Synthetic Spectra

Bell and Gustafsson (1983) have computed synthetic spectra for models with T_{eff}, surface gravity, and metallicity in the range covered by globular cluster stars. Some additional calculations were made for the present paper, using their methods and programs. Line absorption from the relevant molecular bands of CH, CN, NH, and CO as well as atomic lines are included in these spectral syntheses, details of the sources of these data being given by Bell and Gustafsson (1978).

The theoretical molecular band indices were calculated for $T_{eff} = 4000$, 4500, and 5000 K for $Z = 1/3$, 1/10, and $1/100Z_0$ at surface gravities which for each T_{eff} corresponds to those of globular cluster giants. A number of additional models were computed for lower gravities in order to study the abundances of AGB stars, and some further models were computed using nitrogen abundances enhanced by 1 dex. The logarithmic C, N, and O abundances accepted as standard are 8.62, 8.00, and 8.86, on the scale with log $N(H) = 12.0$. Calculations have been carried out using these values and a variety of other values. In particular, we have carried out the calculations for reduced C and O abundances, allowing the N abundance to increase as a result of assumed CN and ON processing. Clearly, the conclusions of the previous section suggest that both CN and ON processed material have been brought to the stellar surface. Synthetic spectra in the 2 μm to 2.5 μm region were used to interpret the PFCAM CO data. Similar calculations were used by Bell, Dickens, and Gustafsson (1979) to check carbon abundances in the M92 stars. Infrared synthetic spectra were computed for the models with $[N/A] = 1.0$ dex, to check the effect of CN absorption on the infrared CO band photometry.

The synthetic spectra covering the ultraviolet and visible spectral regions were flattened in a manner identical to the treatment of the observations, and the molecular band indices and pseudo-equivalent width for Ca I 4226 Å were determined following the prescriptions in § II. In general, because of possible continuum slope problems, it is most reliable to use these theoretical indices differentially to estimate relative abundances between different groups of ω Cen stars. The deduced absolute abundances are least reliable for the Ca I feature, and more reliable for the molecular features. Some tests of the reliability of synthetic spectra computations of similar indices can be found in Bell (1984).

The solid lines in Figures 1 through 7 represent the predicted feature strengths from synthetic spectra for $Z = 1/100$ and 1/10 of Z_0, and, as discussed above, the lowest metallicity group of ω Cen stars is assumed to have $Z = 1/100Z_0$, the intermediate

metallicity group to have $Z = 1/30Z_0$, and the highest metallicity group to have $Z = 0.1Z_0$. The CNO abundances have been assumed to scale with the overall abundances.

The calculated indices are given in Table 4.

b) Atomic Features

We look first at the atomic line features. Although there are problems in defining the continuum shape over a 60 Å bandpass in the blue, the behavior of the observed H + K Ca II index in the ω Cen giants is reproduced reasonably well as a function of T_{eff} within each metallicity group by the predicted indices from the synthetic spectra. The difference between the low and high abundance groups of ω Cen stars appears to be reasonably close to the factor of 10 assumed here. The same is true of the 4226 Å feature of Ca I. The Ca I line is a better abundance indicator in stars which are more metal-rich than the majority of those discussed here. The zero point shift between the observations and the calculations may be due to the sharpness of the Ca I line itself (as sampled by 0.4 Å pixels) and to the narrow bandpasses which may not fairly sample the fluctuating background of weaker absorption lines.

The Ca I index is slightly dependent on the carbon abundance, owing to the CH lines occurring in the feature and continuum bands, but this effect appears to be too small to explain the effect seen in Figure 7. The continuum depression caused by the CH and CN bands in the carbon stars is extremely large (cf Bell and Dickens 1974, Fig. 6), and a completely new calibration is necessary before metallicities can be derived for them.

It is extremely interesting that there is a noticeable tendency for the weak CO stars to have stronger atomic features than their strong CO counterparts within each metallicity group. This effect appears in both the H + K Ca II index and the 4226 Å Ca I line, and corresponds to an enhancement of about 0.5 dex. We will return to this point later.

c) Molecular Features

PFCAM deduced that the difference in the CO indices between CO strong and CO weak stars at a fixed T_{eff} and metallicity corresponds to a C depletion of 0.8 dex, for a fixed O/Z ratio. A carbon depletion of this magnitude is seen in the most luminous stars in M29 and in NGC 6397. However, if the oxygen abundance is constant, the maximum difference in C abundance from the lack of an obvious separation in CH indices between the two groups of stars is 0.4 dex, which is not enough to produce the two separate CO sequences. Frogel, Persson, and Cohen (1981) suggested that the extremely strong violet CN bands seen in the CO weak stars may result in the red system CN bands in the infrared reducing the observed CO indices by a few hundredths of a magnitude. This very interesting suggestion was based upon inspection of calculations of CN line absorption in the 2 μm region and studies of high-resolution spectra of α Boo and β And. It was suggested that the depletion of C and enhancement of N may together be adequate to explain the separation of CO indices. In order to check this hypothesis, we carried out detailed synthetic spectrum and model atmosphere calculations. Models were computed for $[A/H] = -1.0$ and -2.0 dex, with the nitrogen abundance enhanced by 1.0 dex. Infrared synthetic spectra were then computed for these models, again with the high nitrogen abundance. This increase in CN does increase the red CN line absorption in the CO comparison filter band, to about 0.5 mag for the model 4000/0.9/−1.0, but a similar increase in

TABLE 4

COMPUTED INDICES FROM SYNTHETIC SPECTRA

Model (T_{eff}, log g, [Fe/H])	NH (%)	LoCN (%)	CN38 (%)	CN42 (%)	CH (%)	C_2 (%)	CO (mag)	Ca I (Å)	H + K (%)
A. Normal C, N, O									
4000, 1.25, −0.5......	0.183	+0.627	0.676	+0.160	0.254	−0.007	0.172	6.55	0.558
4500, 2.25, −0.5......	0.128	+0.535	0.570	+0.130	0.265	+0.008	0.116	4.48	0.432
5000, 3.00, −0.5......	0.191	+0.358	0.403	+0.067	0.250	+0.010	0.074	3.35	0.424
4000, 0.90, −1.0......	0.190	+0.538	0.590	+0.116	0.250	−0.011	0.150	5.12	0.503
4500, 1.80, −1.0......	0.229	+0.385	0.441	+0.070	0.258	−0.003	0.100	3.56	0.412
5000, 3.00, −1.0......	0.191	+0.206	0.249	+0.026	0.243	−0.002	0.049	2.69	0.412
4000, 0.50, −2.0......	0.206	+0.215	0.244	+0.017	0.210	−0.012	0.099	2.53	0.426
4500, 1.50, −2.0......	0.212	+0.060	0.114	+0.005	0.236	−0.010	0.046	2.06	0.409
5000, 2.50, −2.0......	0.130	−0.001	0.028	+0.004	0.186	−0.004	0.013	1.30	0.415
B. [C, N, O/Fe] = −0.1, +0.26, 0.0 dex									
4000, 1.25, −0.5......	0.173	+0.654	0.686	+0.132	0.245	...	0.164		
4500, 2.25, −0.5......	0.217	+0.606	0.610	+0.130	0.258	...	0.105		
5000, 3.00, −0.5......	0.222	+0.487	0.499	+0.082	0.246	...	0.064		
4000, 0.90, −1.0......	0.184	+0.581	0.612	+0.094	0.237	...	0.147		
4500, 1.80, −1.0......	0.239	+0.484	0.506	+0.069	0.245	...	0.093		
5000, 3.00, −1.0......	0.230	+0.339	0.363	+0.032	0.236	...	0.043		
4000, 0.50, −2.0......	0.298	+0.240	0.249	+0.006	0.198	...	0.095		
4500, 1.50, −2.0......	0.312	+0.127	0.174	−0.004	0.221	...	0.040		
5000, 2.50, −2.0......	0.217	+0.012	0.038	−0.004	0.166	...	0.011		
C. [C, N, O/Fe] = −0.2, −0.6, −0.1 dex									
4000, 1.25, −0.5......	0.187	+0.675	0.694	+0.168	0.245	...	0.152		
4500, 2.25, −0.5......	0.225	+0.652	0.639	+0.176	0.258	...	0.096		
5000, 3.00, −0.5......	0.239	+0.555	0.548	+0.126	0.244	......	0.056		
4000, 0.90, −1.0......	0.200	+0.616	0.631	+0.131	0.237	...	0.134		
4500, 1.80, −1.0......	0.253	+0.551	0.553	+0.110	0.243	...	0.084		
5000, 3.00, −1.0......	0.253	+0.412	0.424	+0.057	0.232	...	0.037		
4000, 0.50, −2.0......	0.335	+0.292	0.296	+0.029	0.197	...	0.087		
4500, 1.50, −2.0......	0.358	+0.198	0.240	+0.010	0.216	...	0.034		
5000, 2.50, −2.0......	0.287	+0.036	0.059	−0.001	0.152	...	0.009		
D. Lower Gravity AGB Models									
4500, 1.50, −1.0......	0.217	+0.432	0.473	+0.043	0.246	...	...		0.445
5000, 2.25, −1.0.....	0.182	+0.207	0.263	+0.019	0.231	...	...		0.427
4500, 0.75, −2.0......	0.163	+0.044	0.098	+0.009	0.178	...	...		0.431
5000, 2.25, −2.0......	0.129	+0.008	0.031	+0.005	0.158	...	...		0.420

line absorption occurs in the CO filter band itself. These synthetic spectra calculations were made using Spindler's (1965) Franck-Condon factors, which agree quite well with the values found by Sneden and Lambert (1982) for the 0–2 and 1–3 bands in the solar spectrum. Although this hypothesis is not borne out by detailed synthetic spectra calculations for normal giants with very depleted C and O and enhanced N, it might be true for CH stars with their very strong CN bands.

The NH feature can be discussed completely separately from the carbon features since the primary depletion of nitrogen is N_2 and not CN. The NH feature shows a strong separation between the CO strong and CO weak ω Cen giants. The CO strong stars appear to have [N/Z] = 0. This separation implies an enhancement of at least a factor of 10 in N/Z (at all metallicities) in the CO weak giants. The greatest values of the NH index are found for the enhanced nitrogen models with [M/H] = −2.0 dex, owing to these models having the lowest line blanketing in the comparison bandpasses.

The CH feature is predicted quite well as a function of T_{eff} by the synthetic spectra. The observed CH indices imply that, if [O/Z] = 0.0, [C/Z] is between 0.2 and −0.5 dex in each of the metallicity groups, and there is no obvious separation between the CO strong and CO weak stars. However, in view of the existence in the CO, CN, and NH features of a clear separation of band strengths between the CO weak and the CO strong stars and the lack of such in the CH band, it is necessary to ask if we can find values of the C and O abundances which give the observed CH band strengths and simultaneously give the N abundance found from the NH bands. Clearly, there is an ambiguity in the carbon abundance found from CH in the absence of knowledge of the oxygen abundance. The lower the oxygen abundance, the lower the carbon abundance can be to match the CH features, since less C is lost via CO formation. Enhancement of nitrogen by 1 dex corresponds to depletion of both C and O by 0.7 dex. We consequently computed synthetic spectra using these abundances.

The 4200 Å CN index is matched reasonably well in the CO strong stars by C/Z × N/Z ratios of 1 to 3. However, in the CO weak stars, the 4200 Å CN band is extremely strong. Given that the C abundance is constrained by the CH indices,

an increase in the ratio of N/Z of between 10 and 30 at all metallicities is derived from the fits to the CN observations of the CO weak giants in ω Cen. This nitrogen enhancement is in excellent agreement with the N enhancements seen in NH and found earlier (Dickens and Bell 1976).

The behavior of the 3880 Å CN band shown in Figure 4 a–c is similar. A separation of about a factor of 10 in N/Z exists between the low CO, strong CN stars, and the strong CO, normal CN stars. The absolute normalization is correct for the low and intermediate metallicity groups in that the mean strength of the 3883 Å CN band is close to that predicted for C/Z and N/Z = 1. In the highest metallicity group of ω Cen giants, the observed molecular indices for the CO strong stars are somewhat below those predicted for N/Z and C/Z = 1; the separation in CN between the CO weak and CO strong stars is still clear.

d) Summary of C and N Abundances

There are three groups of ω Cen giants: the four carbon stars; the group of stars with weak CO, strong NH, and strong CN; and the group of stars with strong CO, weak NH, and weak CN for their metallicities. The atomic and molecular lines are consistent with the weak CO stars having depleted carbon and oxygen, N/Z = 10 to 30, and heavy element metallicities (Z) which are 3 times larger than the strong CO stars at a given position in the H-R diagram. We denote these two groups as the N-enhanced and N-normal stars. If Z of the N-enhanced stars is actually higher, C/Z = $\frac{1}{4}$ to $\frac{1}{2}$ and N/Z = 5–15 among this group.

V. DISCUSSION

a) The N-Enhancement Problem

In the previous section, we demonstrated that there are two groups of giants in ω Cen, the N-enhanced and the N-normal giants, as well as four carbon stars. In order to produce the N-enhanced stars from the N-normal stars, it is necessary that both C and O be depleted. Note that this hypothesis requires that the [O I] lines in the spectra of such stars as RGO 253 should be invisible, consistent with the upper limit of 25 mÅ of Cohen (1981). If the oxygen abundance is constant, the CH indices permit a maximum range in C abundance of a factor of 2. If one assumes C/N in the unmixed stars to be twice solar and that half of the C is burned to N, a nitrogen enhancement factor of 6 can be obtained. But some of the N-enhanced stars have N augmented by a factor of 15; this high degree of N enhancement cannot be produced by CN burning alone, but must involve ON burning and subsequent mixing (see Sweigart and Mengel 1979). For the most extreme N-enhanced stars, it may not be possible to burn C and O into N in adequate quantities without excessively weakening the CN bands below those observed. This problem of an excessive degree of N enhancement is not unique to ω Cen; it has been found in chemically homogeneous globular clusters such as NGC 1851 (Hesser et al. 1982), which contains stars apparently identical to RGO 253, and in M92 and M15 (see the extensive discussion in Carbon et al. 1982; Trefzger et al. 1983; Suntzeff 1981).

b) The Ca Enhancement Problem

In § IV we have shown that the N-enhanced ω Cen giants also apparently have Ca abundances a factor of 3 higher than the N-normal stars with the same position in the H-R diagram. It is possible that these stars represent the more metal-rich ones within each metallicity group. But this then suggests that a slight heavy metal enhancement greatly increases the probability of mixing at a given luminosity (which may also depend on the rotation rate of the stellar core). Given the presence of a significant fraction of unmixed stars even in the highest metallicity group, this cannot be true. Is the slight Ca enhancement produced during the mixing? All calculations of stellar evolution vehemently deny this, but mixing calculations are notoriously difficult and have not met the test of detailed confrontation with observations well in the past. It is also possible that the very strong CN bands in the N-enhanced stars have affected the continuum placement in these moderate-resolution spectra. Our carbon star spectra clearly show such effects, and only higher resolution data can eliminate this possibility for the less extreme cases.

Another hypothesis is that the apparent Ca enhancement in the N-enhanced stars is not real and is due to our inability to separate asymptotic giant branch (AGB) from first-ascent red giants in ω Cen. Because of the range in heavy element metallicity from star to star within ω Cen, AGB stars cannot be picked out via their offset from the first-ascent giants in a color magnitude diagram. Thus AGB stars, which will be systematically bluer in the H-R diagram than normal first-ascent GB stars, will have their $R(V-K)$ indices underestimated by 0.15 to 0.3, based on the large collection of globular cluster photometry by Frogel, Persson, and Cohen (1983). They will therefore appear to have systematically enhanced element line strengths compared to the normal GB stars in the same range of $R(V-K)$.

The AGB stars will also have lower surface gravities than the GB stars due to mass loss during the He flash and to the luminosity difference between the AGB and the RGB. The surface gravity difference at a fixed T_{eff} can be as large as 0.5 dex. Those features which, in the relevant range of T_{eff}, become stronger for lower gravities, such as H + K of Ca II (see Bell 1985; Suntzeff 1981), will be enhanced in the AGB stars: the enhancements shown in Table 4 are not very large but may be adequate.

The suggested identification of the N-enhanced stars as mixed AGB giants eliminates the apparent heavy element enhancement, and it solves the problem of when doe the mixing event take place (i.e., during the He flash). The detailed abundance analyses of ω Cen giants such as those of Cohen (1981) do not yet cover a large enough sample to decide whether the apparent Ca enhancements seen in our moderate-resolution data are real. Cohen (1981) found a general large enhancement of Ca/Fe, as is typical of metal-poor halo stars. Her mean [Ca/Fe] of 0.7 dex may be an overestimate, since the very precise calcium oscillator strengths of Smith and Raggett (1981) are, on average, 0.18 dex larger than the values she used. Cohen found a range in Ca/Fe from star to star within ω Cen of about a factor of 2, but whether this is dominated by errors in the analysis and whether the increase in Ca/Fe correlates with N enhancement is not yet clear.

Is the suggested identification of the N-enhanced stars as AGB stars reasonable based on their relative numbers? The Cannon and Stobie (1973) unbiased sample of confirmed proper motion ω Cen giants with $B-V > 0.85$ mag and $11 < V < 13$ mag consists of 47 stars, 60% of which were observed by PFCAM and also are included here. All the reddest stars ($B-V > 1.4$ mag) in the unbiased Cannon and

Stobie sample were included here; the fraction of very red stars ($B-V > 1.5$ mag) in the unbiased survey is less than 10% of the total, but is about 40% of the present sample. Thus there is tendency to skew the abundance distribution toward higher abundance ω Cen stars [i.e., those with large values of $R(V-K)$]. However, the small difference in luminosity between first and second ascent giant branch stars at a given color should lead to a sample essentially unbiased in its ratio of GB to AGB stars. About 40% of the unbiased sample where discrimination is possible belong to the CO weak, N-enhanced stars. This is a reasonable fraction for the ratio of second to first-ascent red giants near the red giant tip, although the expected fraction falls rapidly as one descends in luminosity down the giant branch (see Green 1981). Selection effects in our sample preclude use of a luminosity function to further test this hypothesis.

c) Comparison with Other Clusters

There is a large body of data on CN and CH variations among the "chemically homogeneous" globular clusters. The existence of a range of CN band strengths or a bimodel distribution of CN band strengths at a given T_{eff}, has been widely noted (see, for example, Dickens, Bell, and Gustafsson 1979; Norris and Smith 1983; Smith and Norris 1983 and references therein, as well as the work of the Lick group cited earlier in § Va). The much smaller range in CH band variations than in the variation in strength of the 3883 Å CN band is also a common theme of these studies. The main difference at first sight is that the N enhancements in many clusters are claimed to be independent of whether a star is a first or second-ascent red giant, and of how close to the giant branch tip it may be. In ω Cen, it is still plausible that the N-enhanced stars are AGB stars.

AGB stars are expected to reside on the blue side of the giant branch. The N-enhanced stars in NGC 1851 (Hesser et al. 1982) show no tendency to do so. Nor is such an effect seen within each metallicity group of ω Cen giants. Thus the hypothesis presented in § Vb that the N-enhanced stars in ω Cen are AGB giants may not in fact be correct. Analogy to other globular clusters such as M92 (Carbon et al. 1982) (see also § Vc) where such N-enhanced stars have been seen on the subgiant branch below the minimum luminosity of the AGB also suggests that the N-enhanced stars are not all AGB stars. Lower luminosity stars in ω Cen and in other globular clusters must be studied to understand the origin of the N-enhanced stars.

There have been several claims of correlations of enhanced Ca with enhanced CN in clusters traditionally viewed as chemically homogeneous. These are summarized in Norris and Freeman's (1983) extensive analysis of about 100 red giants in M22. They find a wide range in CN strength and also a range in H+K Ca II line strength, correlated with CN, at a given color. They assert that their M22 sample has fewer than 10% AGB stars, based on the ratio of AGB stars to red giants at magnitudes just above the horizontal branch where the first and second-ascent red giants are well separated in H-R diagrams. However, the luminosity function for first and second-ascent red giants is very different (see, for example, Iben and Truran 1978), and substantial AGB contamination at higher luminosities can be expected.

A clear separation of first-ascent red giants from AGB stars is particularly difficult in M22 because of the large reddening and its spatial variation (see Cohen 1981) over the face of the cluster. This produces an H-R diagram whose sequences are neither tight nor cleanly separated. Could the N-enhanced, Ca rich M22 stars be AGB giants and the Ca enhancement be only an artifact? The N-enhanced stars in M22 again tend to be on the red side of the giant branch, which is the opposite of that expected for AGB stars.

d) The C Stars

The five C stars known to be members of ω Cen require a separate mixing event from the N-enhanced giants. Since all the carbon stars are brighter than the horizontal branch, one may assume they are AGB stars which have undergone mixing of C formed by triple-α reactions. Their luminosities are too low for thermal pulses to have occurred, and no satisfactory theoretical explanation exists for carbon stars of such low luminosity. Two C stars are also known in M22 (McClure and Norris 1977; Hesser and Harris 1979) and one in M55 (Lloyd-Evans 1979). It is not yet possible to establish why only certain clusters have C stars. The cluster mass or metallicity are not the determining factor. (See McClure 1979 for further discussion of these objects.)

VI. SUMMARY

Spectral scans of 72 stars in ω Cen have been used to measure the strengths of molecular bands of CH, NH, and CN, as well as atomic lines of Ca I and Ca II. These indices have been combined with the published CO indices and infrared colors of PFCAM and calibrated using identical indices computed from spectra synthesized from model atmospheres of the appropriate T_{eff} and surface gravities using reasonably complete line lists. Because ω Cen has a wide range in heavy element metallicity, the analysis is somewhat complicated. We use a parameter $R(V-K)$ introduced by PFCAM which is based on the position of a star in the H-R diagram with respect to the loci of giants in chemically homogeneous, well-studied globular clusters to separate the ω Cen giants into lowest, intermediate, and highest metallicity groups.

We find (in addition to the four C stars) two groups of ω Cen giants. The N-enhanced group has N/Z enhanced by a factor of 5 to 15, while C may be depleted by a factor not larger than 4 with respect to the N-normal group, which has C/Z and N/Z solar. The N-enhanced stars also have weaker 2.4 μm CO indices and stronger atomic Ca features than the N-normal stars of the same metallicity group and T_{eff}. The very large nitrogen enhancements seen in some of the ω Cen giants require processing of both C and O into N.

Once the effects of the spread in heavy element metallicity within ω Cen have been removed, the pattern of the variations of the light elements within ω Cen is similar to that seen in other globular clusters.

REFERENCES

Bell, R. A. 1984, *Pub. A.S.P.*, **96**, 318.
———. 1985, *Pub. A.S.P.*, **97**, 219.
Bell, R. A., and Dickens, R. J. 1974, *M.N.R.A.S.*, **166**, 89.
———. 1980, *Ap. J.*, **242**, 657.
Bell, R. A., Dickens, R. J., and Gustafsson, B. 1979, *Ap. J.*, **282**, 428.
Bell, R. A. and Gustafsson, B. 1978, *Astr. Ap. Suppl.*, **34**, 229.
———. 1983, *M.N.R.A.S.*, **204**, 249.
Bond, H. E. 1975, *Ap. J. (Letters)*, **202**, L47.
Cannon, R. D., and Stobie, R. S. 1973, *M.N.R.A.S.*, **162**, 207.
Carbon, D. F., *et al.* 1982, *Ap. J. Suppl.*, **49**, 207.
Cohen, J. G. 1978, *Ap. J.*, **223**, 487.
———. 1981, *Ap. J.*, **247**, 869.
———. 1983, *Ap. J.*, **270**, 654.
Dickens, R. J. 1972, *M.N.R.A.S.*, **159**, 7P.
Dickens, R. J., and Bell, R. A. 1976, *Ap. J.*, **207**, 506.
Dickens, R. J., Bell, R. A., and Gustafsson, B. 1979, *Ap. J.*, **232**, 428.
Freeman, K. C., and Rodgers, A. W. 1975, *Ap. J. (Letters)*, **201**, L71.
Frogel, J. A., Persson, S.E., and Cohen, J.G. 1981, *Ap. J.*, **246**, 842.
———. 1983, *Ap. J. Suppl.*, **53**, 713.
Gratton, R. 1982, *Astr. Ap.*, **115**, 336.
Green, E. 1981, Ph.D. thesis, University of Texas at Austin.
Harding, G. A. 1972, *Observatory*, **82**, 205.
Hesser, J. E., Bell, R. A., Cannon, R. D., and Harris, G. L. H. 1982, *A.J.*, **87**, 1470.
———. 1985, *Ap. J.*, **295**, 437.
Hesser, J. E., and Harris, G. L. H. 1979, *Ap. J.*, **234**, 513.

Iben, I., Jr., and Truran, J. W. 1978, *Ap. J.*, **220**, 980.
Lambert, D. L. 1978, *M.N.R.A.S.*, **182**, 249.
Lloyd Evans, T. 1979, private communication.
———. 1983, *M.N.R.A.S.*, **204**, 975.
Mallia, E. A., and Pagel, B. E. J. 1981, *M.N.R.A.S.*, **194**, 421.
McClure, R. D. 1979, *Mem. Soc. Astr. Italiana*, **50**, 15.
McClure, R. D., and Norris, J. 1977, *Ap. J. (Letters)*, **217**, L101.
Norris, J., and Bessell, M. S. 1975, *Ap. J. (Letters)*, **201**, L75.
Norris, J., and Freeman, K. C. 1983, *Ap. J.*, **266**, 130.
Norris, J., and Smith, G. H. 1983, *Ap. J.*, **275**, 120.
Persson, S. E., Frogel, J. A., Cohen, J. G., Aaronson, M., and Matthews, K. 1980, *Ap. J.*, **235**, 452 (PFCAM).
Shectman, S. 1978, *Carnegie Institution of Washington Year Book*, **77**, 200.
Smith, G., and Ragett, D. St. J. 1981, *J. Phys. B.*, **14**, 4015.
Smith, G. H., and Norris, J. 1983, *Ap. J.*, **264**, 215.
Sneden, C., and Lambert, D. L. 1982, *Ap. J.*, **259**, 381.
Spindler, J. 1965, *J. Quant. Spectrosc. Rad. Transfer*, **5**, 165.
Suntzeff, N. B. 1980, *A.J.*, **85**, 408.
———. 1981, *Ap. J. Suppl.*, **47**, 1.
Sweigart, A. V., and Mengel, J. G. 1979, *Ap. J.*, **229**, 624.
Tomkin, J., and Lambert, D. L. 1984, *Ap. J.*, **279**, 220.
Trefzger, C. G., Carbon, D. F., Langer, G. E., Suntzeff, N. B., and Kraft, R. P. 1983, *Ap. J.*, **266**, 144.
Webbink, R. F. 1981, *Ap. J. Suppl.*, **45**, 259.
Woolley, R. V. d. R. *et al.* 1966, *Royal Obs. Ann.*, No. 2.

ROGER A. BELL: Astronomy Program, University of Maryland, Space Science Building, College Park, MD   20742

JUDITH G. COHEN: 105–24, California Institute of Technology, Pasadena, CA   91125